International Journal of Innovative
Computing, Information and Control
Volume 14, Number 6, December 2018

pp. 2071–2090

DESIGN OF SOLAR CHARGER CHALLENGING VARIOUS SOLAR IRRADIANCE AND TEMPERATURE LEVELS FOR ENERGY STORAGE

Suntiti Yoomak, Chaiyan Jettanasen and Atthapol Ngaopitakkul*

Department of Electrical Engineering
Faculty of Engineering
King Mongkut's Institute of Technology Ladkrabang
Chalongkrung Rd., Ladkrabang, Bangkok 10520, Thailand
*Corresponding author: knatthap@kmitl.ac.th

Received March 2018; revised July 2018

Abstract. *This paper presents the design of a solar charger which charges a lead-acid battery using three charging states: the 1st state is a constant-current charging state which uses a high current, the 2nd state is a constant-voltage charging state which charges the battery until the capacity is 95% in order to save the battery life cycle and the 3rd state is a float-voltage charging state which is used to protect the battery from self-discharging. Using a case study, the three charging stages of the designed battery charger are implemented using an experimental setup: a photovoltaic simulator, a 12-V 60-Ah lead-acid battery, an oscilloscope and a FLUKE 435b power-quality meter. The solar irradiance level and temperature level are varied by using the software of the photovoltaic simulator. The designed battery charger controls a voltage and a current level to charge the battery using pulse-width modulation (PWM) control signals to determine the duty cycle. Experimental results reveal that the control of the battery charging in each charging state is feasible and effective based on the power circuit and the control circuit. The microcontroller is employed to process and control the change of the charging state, which has a suitable voltage and current, hence increasing the lifetime of the battery. The designed battery charger can charge the battery with a maximum current of up to 8 A.*
Keywords: Solar energy, A solar charger, A buck converter, A lead-acid battery

1. **Introduction.** Nowadays, the global energy consumption has rapidly increased, and is expected to result in fossil fuel energy depletion and environmental problems related to CO_2 emissions and global warming. Thus, when addressing this issue, renewable energy has become a more important resource owing to its green energy and abundant available sources. The most popular source of renewable energy is solar energy, which utilizes solar panels to generate electricity from sunlight incident on them. However, the output of a solar panel relies upon environmental factors, irradiance and temperature, which vary throughout any given day. To decrease the fluctuations in the solar energy output, a solar energy system is usually backed up with a battery by using a charger controller.

Typically, a common battery charger is required to control the current to the battery with an optimal rate, and to cease charging when the battery is fully charged. However, for battery charging with solar energy, the input of the solar battery charger is uncontrollable owing to the changing weather conditions. For this reason, conventional battery chargers fail to charge batteries efficiently and safely when using solar energy. A battery charged by solar energy without the optimal input control of a converter is described by Thomas and Nelson [1]. It is shown that battery charging with an unregulated voltage or

DOI: 10.24507/ijicic.14.06.2071

current is a contributing factor in battery damage, and reduces the battery life cycle. The most important function of a battery-management system is the solar battery charger, which consists of a part of a DC/DC converter application which provides the interface between solar energy and the battery, leading to optimal energy transfer [2]. Hence, the DC/DC converter is critical to regulating and transferring a suitable charging voltage and current according to battery specifications. Hussein and Fardoun [3] reported that the main problems encountered in battery charger systems with solar energy are intermittent radiation and temperature during the day, requiring the use of variable input power. Generally, techniques for charging batteries depend on terminal measurements, i.e., the voltage, current or temperature. Hence, the system will cut off the charging battery before it is truly fully charged, resulting in a reduction in the usable capacity.

By considering traditional battery chargers [4-10], Cope and Podrazhansky [5] showed that a constant-current charger is inexpensive to implement. However, it causes overcharging based on its charging process, which has a negative effect on battery performance. A comparison between a constant-current and voltage-charging method, as well as between multiple constant-current and voltage-charging methods was reported by Li et al. [6]. It can be deduced that the use of multiple constant-current and voltage-charging methods with the addition of a negative pulse discharge to eliminate the polarization effect is more efficient than the constant-current and voltage-charging method. To improve the efficiency of battery charging, Guo and Zhang [7] proposed fast charging with a negative pulse-discharge method. The negative effects of battery charging are improved by using constant-current charging and limited voltage charging. Results show that the use of a negative pulse discharge can increase the efficiency of battery charging. There are different battery-charging techniques, which vary in terms of their effectiveness, complexity and ease of implementation. The constant-current charging method, or constant-current and voltage-charging method are simple. However, these techniques affect the failure with respect to the optimal charging rate and overcharging battery, resulting in a decreased life-cycle of the battery [8]. Conventional charger controller approaches are unsuccessful when charging batteries with solar energy in various environmental conditions because of the irradiance level and temperature level. Thus, the paper by Boico et al. [9] discusses and investigates the reasons for failure problems, and introduces charger-control techniques which are based on the voltage and temperature levels. In addition, maximum power-point tracking (MPPT) was also employed by using a microcontroller in order to increase the speed of charging. For battery charging with solar energy, battery-charging control techniques are divided into two classes, which are single-stage and multi-stage techniques. The single-stage technique is less complex than the multi-stage technique. Thus, the latter is most efficient for battery charging [10].

To charge a battery with solar energy [11-17], it is important to keep the energy supply from the solar panel continuous and optimum to prevent energy loss. Hsieh et al. [11] proposed a photovoltaic (PV) burp-charge system which makes a continuous solar energy flow with optimum MPPT, increasing the efficiency of the system. An experimental prototype was used to test the proposed concurrent-charging technique. Results show that the proposed method is feasible for solar energy applications with a battery charger. The non-isolated converter and a transformer isolation converter are a step-up DC/DC converter widely used in solar energy applications [12,13]. Chen et al. [14] discuss an interleaved boost-converter method which is connected in parallel with a DC-link capacitor in each switch. A high-efficiency PV-based battery charger is presented by Fathabadi [15]. A step-up DC/DC converter which consists of one switch and two diodes (hence no switching losses), and an MPPT controller were designed for high efficiency. Experimental results claim that the proposed battery charger method has the highest efficiency of 98.2%

when compared with other traditional battery-charger methods. Moreover, the designed MPPT controller also gives the shortest time for tracking the maximum power compared to other conventional techniques. Then, in order to decrease switching losses, a soft-switching boost converter using two switches and operating in zero-voltage switching mode was reported by Park et al. [16]. Choi et al. [17] presented a two-transformer step-up DC/DC converter approach which includes two switches. The primary sides of both transformers are connected in series; the other sides of the transformers are connected to a DC-link capacitor via a voltage doubler.

A cheaper microcontroller based on the MPPT algorithm for solar-battery chargers was proposed by Koutroulis et al. [18]. With this method, a DC/DC converter is developed using a digital signal processing (DSP) platform, and the results obtained show that the output from the solar panel is increased by 15%. Next, Alberto et al. [19] investigated and developed a solar-battery charger using a microcontroller. The developed charger can increase the output power by 25%, and the MPPT efficiency reaches 95%. Salas et al. [20] present a battery charger that uses solar energy based on a microcontroller design. The designed charger can reduce the overall price because there is more the PV current operation; hence, there is an increase in the efficiency by 18.5%. However, this method needs to improve the efficiency and ensure greater system stability during dynamic conditions. A paper by Khemissi et al. [21] presents a stand-alone solar energy system based on a microcontroller, which has a low cost, high efficiency and good power quality. The system comprises a step-down DC/DC converter to charge a battery using solar energy with MPPT and a single-phase inverter (220 V/50 Hz) with a low total harmonic distortion (THD). A microcontroller PIC 16F876 is selected to design an algorithm which is used to detect the maximum power of the solar energy along with its operation. In addition, the microcontroller is also used to control pulses of the inverter, resulting in decreased inverter losses and a simple filtered output voltage.

Kuo et al. [22] proposed the design of an automatic device for a solar energy harvesting system, and determined its efficiency using the software Visual Basic. A synthesis of the devices used in this research technique results in a shortened design time. Moreover, the data generated by the solar-energy harvesting system is recorded using a smart meter system which was developed to measure its information on an online system. Thus, the data of the system can be provided to users at any time and from anywhere. A battery solar charger for lead-acid batteries using a step-down DC/DC converter with a digital control strategy was developed by López et al. [23]. A DSP was used to control the state of charging, and there are three charging states. In addition, an incremental conductance MPPT technique was implemented. Next, Eldahab et al. [24] developed an MPPT controller with a microcontroller-based battery charger, which provides constant-current and constant-voltage charging to decrease the charging period of a battery. Based on experimental results, the developed controller can track the maximum power point faster than common-controller techniques, and the charging time is also decreased.

By reviewing the many above-mentioned articles involving battery charging with solar energy, it was found that different types of control of DC/DC converters have been studied and applied to develop battery chargers which use solar energy [4-10]. Various techniques for battery charging with solar energy are reported, including constant-current charging, constant-voltage charging and on-off charging. However, the output power efficiency is low since they cannot instantaneously respond to intermittent solar energy, resulting in battery life-cycle reduction. In [11-17], the various DC/DC converter design and battery charging with the MPPT technique for solar energy were discussed. These approaches can improve conversion efficiency and maintain the life-cycle of batteries. Next, [18-24] proposed incorporating the art of state control with a microcontroller to control voltage and/or the voltage of a DC/DC converter by adjusting the duty cycle, providing high efficiency and good power quality. However, they necessitate more complex circuit control with complicated algorithm.

In this study, the solar charger design for lead-acid battery charging uses three charging states. The first state is a constant-current charging state, the second state is a constant-voltage charging state and the last state is a float-voltage charging state. The three-stage charging process of the designed battery charger is implemented using an experimental setup comprising a PV simulator, a 12-V 60-Ah lead-acid battery, an oscilloscope and a FLUKE 435b power-quality meter. The designed battery charger controls the voltage and current levels to charge the battery using the control signals from the microcontroller to determine the duty cycle. Moreover, the irradiance level and temperature level are varied using the software of the PV simulator to test the designed solar charger efficiency. The paper is organized as follows. Section 2 discusses the proposed solar charger design method. Then, the experimental setup design is proposed in Section 3. The experimental results are presented and discussed in Section 4, and Section 5 concludes the paper.

2. **Solar Charger Design Method.** A schematic block diagram of a battery charger controller is illustrated in Figure 1(a). A PV panel acquires solar irradiance from the sun, after which it then generates electrical energy as a DC current. The DC current flows into a buck converter (DC/DC converter) to convert the level of voltage for battery charging. The battery used is a 12-V lead-acid battery that requires 14 V to maintain reasonable charging rates. Analog signals of voltage and current from the output of the buck converter are detected using the signal detector of a microcontroller to process and send control signals (PWM) to the buck converter.

The configuration of the proposed solar energy battery charger, which consists of a voltage regulator, a metal-oxide semiconductor field-effect transistor (MOSFET) drive, a buck converter, a current detector, a voltage detector and a microcontroller is illustrated in Figure 1(b). Figure 2 depicts the voltage regulator circuit. The voltage regulator is comprised of 5-V and 12-V outputs. The 5-V output is fed to IC LM7805 to provide power for the microcontroller and current detector. The 12-V output is used for IC LM2575-12 to supply the MOSFET driver. Figure 3 shows the components of the MOSFET driver circuit, while Figure 4 shows the buck converter circuit.

By considering Figure 2, the PV panel generates voltage to supply the voltage regulator through capacitor (C1) and capacitor (C2), which are used for voltage regulation. The voltage is delivered to IC LM2575-12 to convert it to 12 V via the inductor (L1) which is required to reduce the distortion problems of currents before the voltage is provided for the MOSFET driver. After that, the voltage of 12 V is sent to IC 7805, and is used to change the voltage to 5 V via the capacitor (C3) to attain a smooth voltage. Further, the capacitor (C4) and capacitor (C5) are installed in order to control the voltage level before it is supplied to the microcontroller and the current detector.

By considering the components of a MOSFET driver circuit, as shown in Figure 3, the circuit receives the 12-V voltage which is supplied from the voltage regulator through the capacitor (C1) and capacitor (C2) to perform voltage regulation, and it is then fed into the IR2101 at the Vcc and Vb inputs. IC IR2101 with 8 channels is used to assemble the MOSFET driver. PWM control signals from the microcontroller are sent to the Hin input of the IR2101. The IC receives duty-cycle signals which are generated from the microcontroller, and amplifies the signals before sending them to drive the MOSFET. The output Ho is the PWM control signal which increases the voltage by using the resistor (R1) to limit the current.

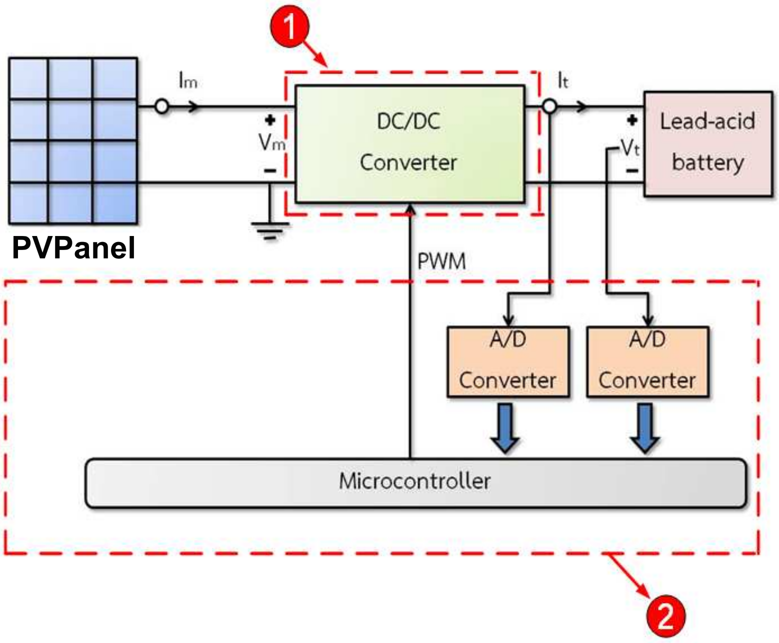

(a) Schematic block diagram of a battery charger controller

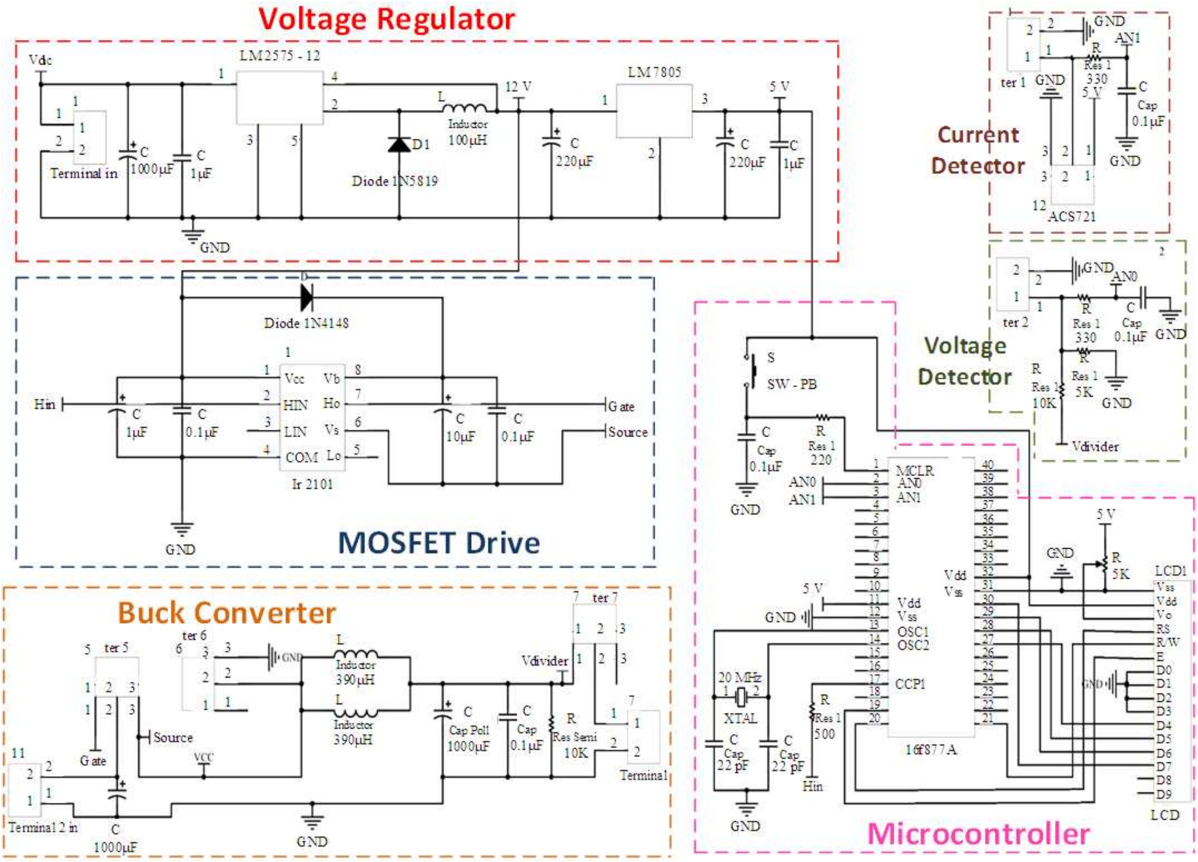

(b) Schematic circuit of a solar energy battery charger

FIGURE 1. Solar energy battery charger

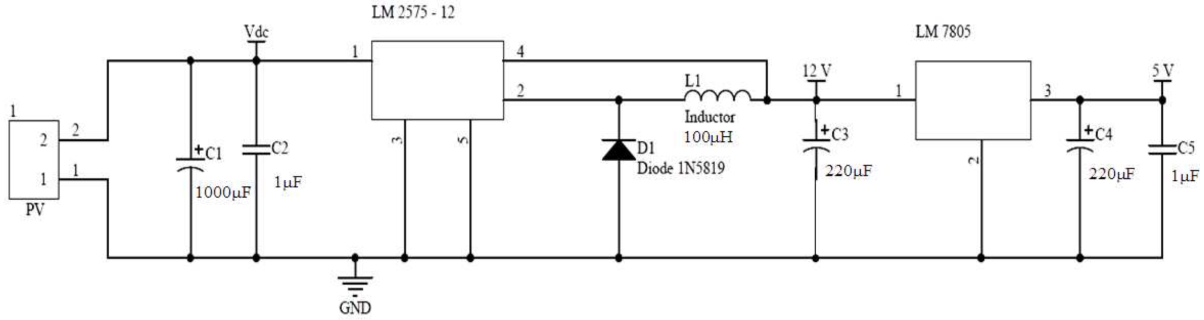

FIGURE 2. Schematic diagram of the voltage-regulator circuit

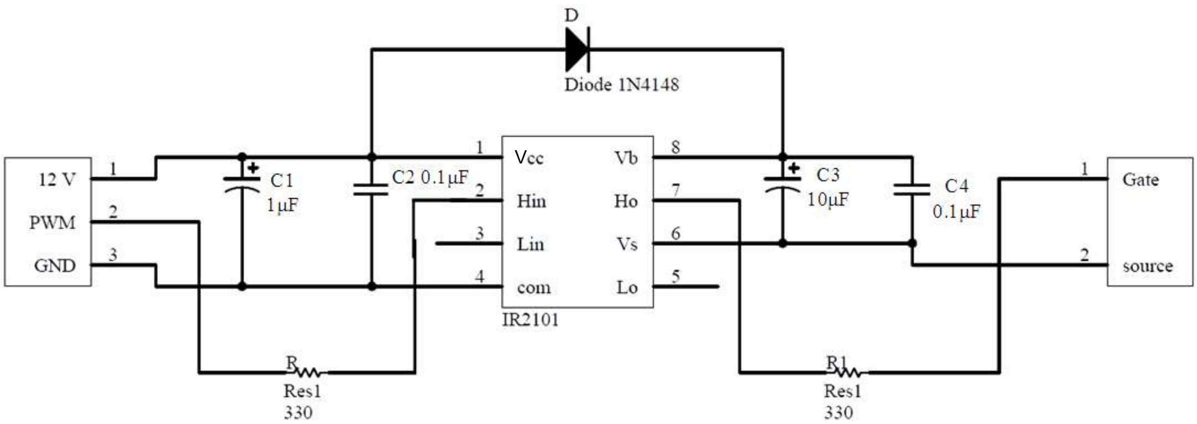

FIGURE 3. Schematic diagram of a MOSFET driver

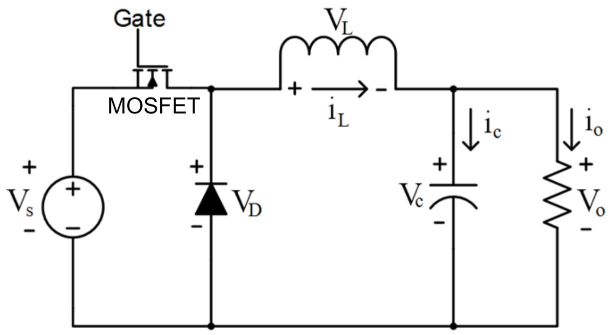

FIGURE 4. Buck converter circuit

The current and voltage output of the PV panel are detected, and are sent to the microcontroller.

– An ACS712 sensor which is a 20 A maximum current is used to detect currents.

– Voltage detection is carried out by applying the principle of voltage dividers.

The analogue signals of the currents and the voltage output of the buck converter are delivered to the microcontroller (PIC16F877A) which is used to process and control the battery charger controller.

By considering the circuit of the buck converter as shown in Figure 4, the MOSFET is switched by using PWM control signals from the microcontroller. A diode is a device which allows a continuous electrical current flow to a load when the MOSFET is switched off. An inductor and a capacitor are used to transfer power from the input to the output. The buck converter used in the experimental model is comprised of the following elements:

– the capacitor is a high-pass filter with an inductor at the output, and provides an electrical current to a load;
– the MOSFET has a switching device which uses control signals: power MOSFET IRF 2807;
– the inductor has a load supply, a current filter and protection of current spikes: an EE ferrite core which has low-loss energy;
– the diode used is NSD318 b20100G.

By considering Figure 5, the voltage of the battery is first checked to determine the battery-charging conditions, which are a constant-current charging state, a constant-voltage charging state and a float-voltage charging state. When the battery is charged with the constant-current charging state, the control program will detect the voltage. If the voltage reaches the determined value, the battery will enter the constant-voltage charging state. When the charging current decreases to 0.1 A, it is moved to the last state of charging, i.e., the float-voltage charging state. Figure 6 shows the relationship between the voltage and current while a battery is charging. The microcontroller is used to perform the process according to Figure 5.

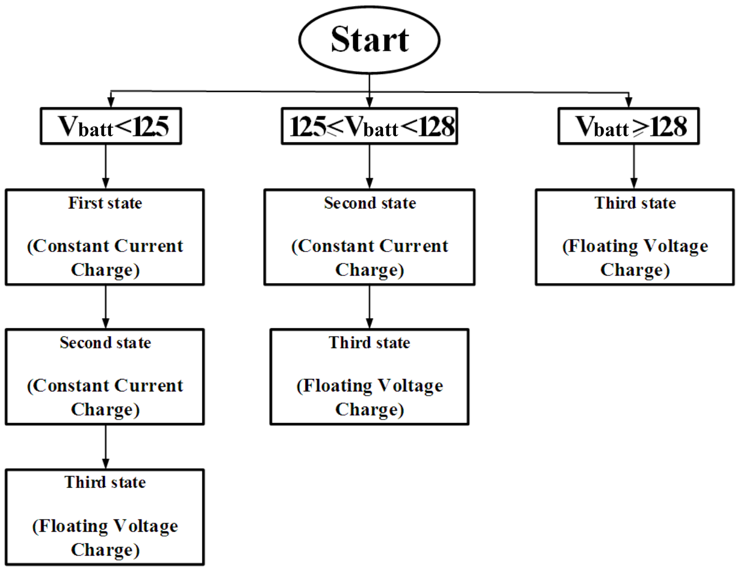

FIGURE 5. Flowchart of a battery-charger controller

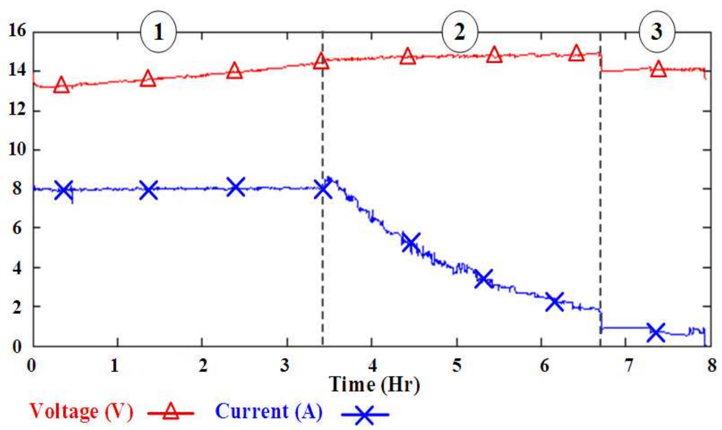

FIGURE 6. Relationship between the voltage and current while the battery is charging

3. **Experimental Setup Design.** The designed solar energy battery charger was tested in a laboratory, and a single-line diagram of the experimental setup is shown in Figure 7(a), while the experimental setup is shown in Figure 7(b). The experimental setup is comprised of a three-phase AC source (denoted by number 1), a PV simulator (denoted by number 2), the designed battery charger (denoted by number 3), a junction box (denoted by number 4), a 12-V 60-Ah lead-acid battery (denoted by number 5), an oscilloscope (denoted by number 6) and a FLUKE 435b power-quality meter (denoted by number 7).

By considering Figure 7, the PV simulator receives electrical energy from the AC source in the laboratory. The electrical energy generated from the PV simulator can be set using software, depending on the irradiance and temperature level. The solar panel in the PV simulator was chosen as poly crystalline silicon with a maximum power of 160 W, a maximum voltage of 34.6 V, a maximum current of 4.60 A, a short-circuit current of 5.1 A and an open-circuit voltage of 42.8 V (the parameters are set at 1000 (W/m^2), while the temperature is set at 25°C). Figure 8 shows the I-V curve characteristics of the solar panel used in the experiment. The designed battery charger controls the voltage

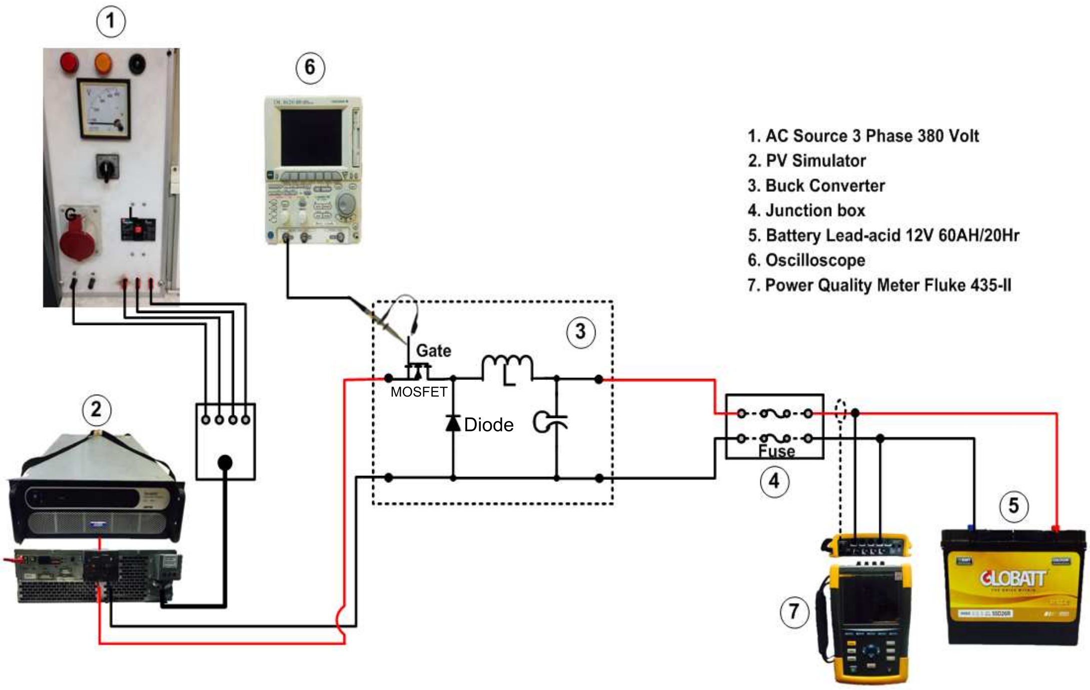

(a) Single-line diagram of the experimental setup

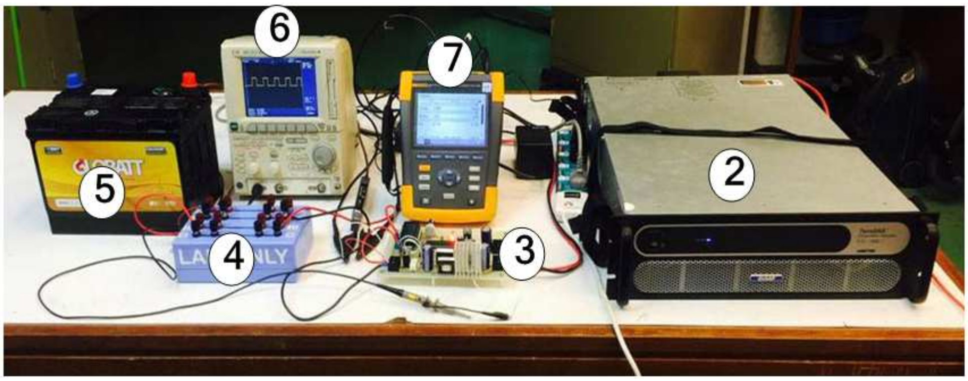

(b) Experimental setup

FIGURE 7. Experimental setup of the solar energy battery charger

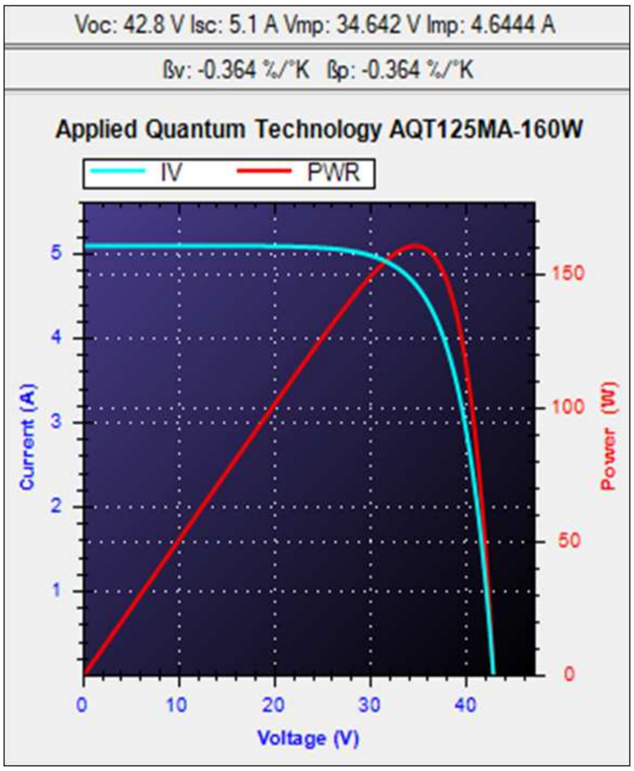

FIGURE 8. I-V curve characteristics of the solar panel

level to charge the battery by using PWM control signals to determine the duty cycle. The oscilloscope was employed to detect the PWM control signals. The power-quality meter was used to measure and record electrical parameters: voltage (V), current (A) and active power (P). Experimental results of the battery charging with three charging states are as follows: the constant-current charging state, constant-voltage charging state and float-voltage charging state are presented, while the results for the battery charger are presented to evaluate the relationship between the irradiance level, temperature level, and the duty cycle.

4. **Experimental Results and Discussion.** As illustrated in Figure 5, the constant-current charging state is the first state of charging the battery. The current of the charging battery is limited to approximately 8 A, and its voltage is approximately 14.6 V. When the battery terminal voltage reaches 14.6 V, the second state of charging the battery (the constant-voltage charging state) is employed. The voltage of the battery charging is continuously limited to about 14.6 V. When the charged current decreases to 1.5 A, the last charging state was employed, and the designed battery charger shifts to the float-voltage charging state. The designed battery charger was tested to evaluate the relationship between the irradiance level, temperature level and duty cycle.

Figure 9 presents the solar irradiance level and temperature when charging the battery. It was found that solar irradiance levels are high for the period 120-300 min, resulting in greater power generation. However, during that period, the temperature is relatively high, and has a negative effect on the voltage output of the solar panels. Figure 10 shows the current, voltage and active power values of solar-energy generation based on the solar irradiance and temperature conditions shown in Figure 9, while the current, voltage and active power values of the charging battery with the designed solar charger are shown in Figure 11.

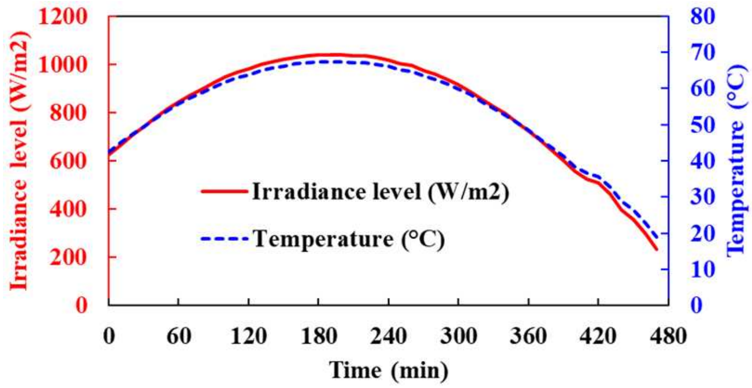

FIGURE 9. Solar irradiance level and temperature used in the experiment

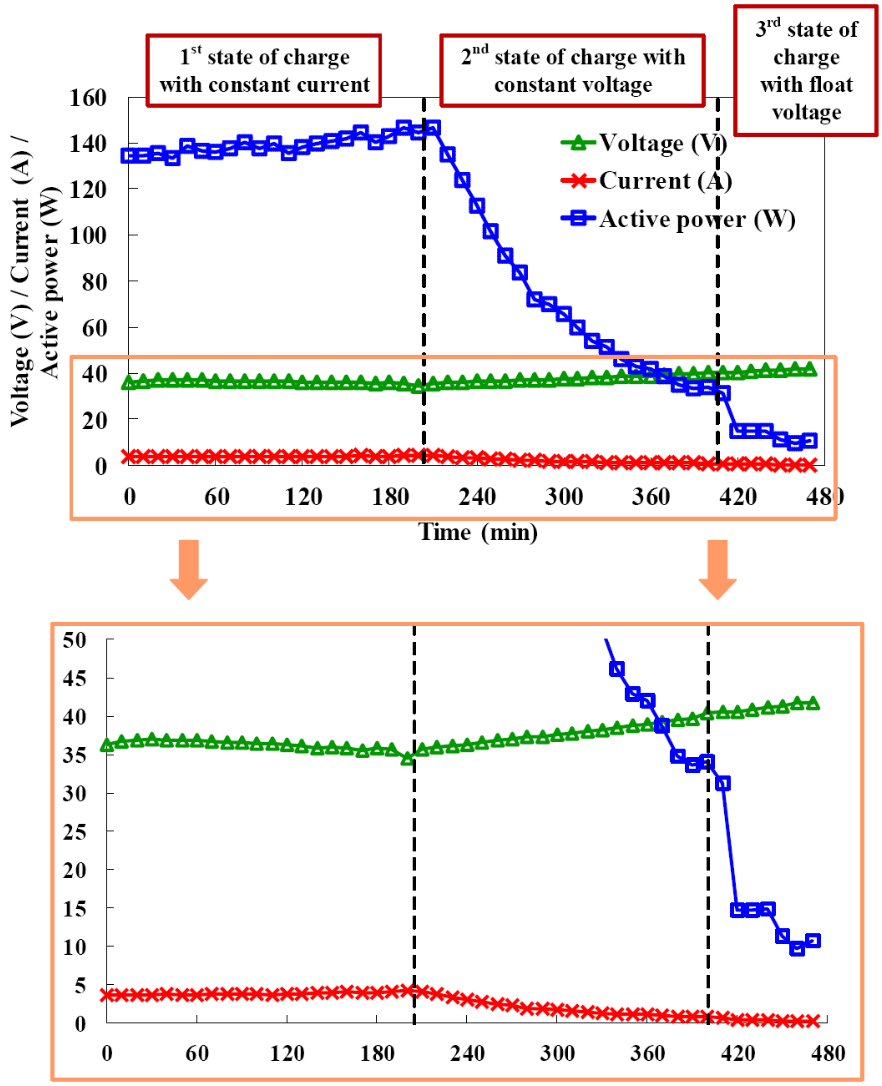

FIGURE 10. Electrical parameters of solar-energy generation

From Figure 10, the power generated from solar energy is dependent on the solar irradiance levels, the temperature as well as the connected load, which is the battery charging in each state. In the 1st state, the solar energy can produce a reactive power of about 130-145 W, a current of about 3.7-4.1 A, and a voltage of approximately 36 V.

During the 2nd and 3rd states, the active power and current of the solar energy tend to decrease, and rely on the battery capacity, whereas the voltage slightly increases. However, it was found that the voltage from the solar energy is not appropriate for directly charging the battery, which is a 12-V 60-Ah lead-acid battery. Hence, a solar battery charger is necessary.

From Figure 11, in the 1st state, based on the constant-current charge, it is shown that the designed charger can vary the voltage and current with optimal values to charge the battery, and achieves a voltage of about 13-14.4 V, and a stable current charge of 8 A. Thus, there is a charging power of about 110-115 W and an efficiency of 80% compared to the active power generated from the solar energy. Then, when the battery is charged to have a capacity of 80%, the constant-voltage charging is activated. The switch from the 1st state to the 2nd state takes place seamlessly when the battery reaches the set voltage limit of 14.6 V. The current and active power begin to drop because the battery starts to become saturated. In this state, the efficiency is 88%. Although the 2nd state needs to take the slower constant-voltage charge that lasts for another 3-4 h, it is important for the well-being of the battery. If the battery is charged without the constant-voltage state, it eventually loses its ability to accept a full charge, and the performance will decrease. When its capacity is charged up to 95%, the 3rd state, which is the float-voltage charge, is

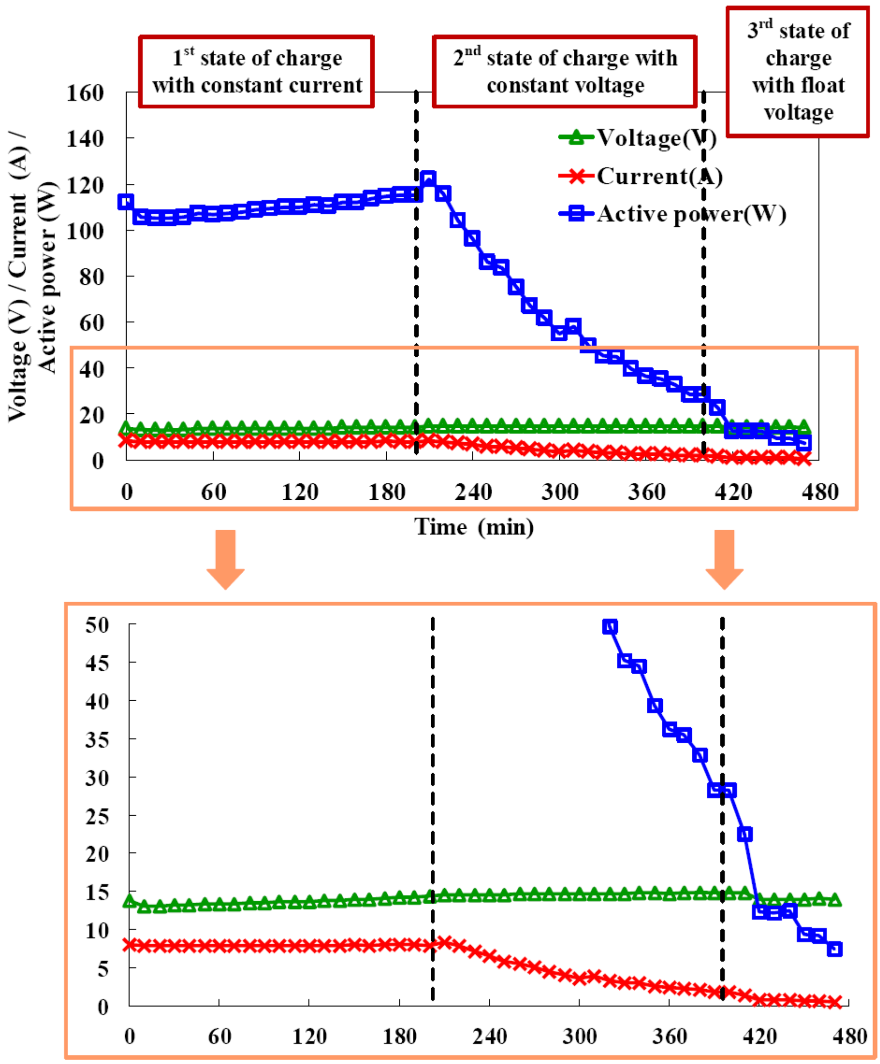

FIGURE 11. Electrical parameters of solar battery charger

used to maintain the battery at full charge with an efficiency of 83% by setting a constant voltage of 13.8 V. If the battery is fully charged, the current will drop to a predetermined low level and the float voltage will also be reduced.

As mentioned above, the designed charger can keep the power generated from solar energy based on various environmental conditions to charge the battery with high efficiency during all of the charging processes. This section discusses the effects of solar irradiance and temperature on the designed battery charger control based on the duty-cycle adjustment in each state of battery charge (1^{st} state of charge with a constant current, 2^{nd} state of charge with a constant voltage and 3^{nd} state of charge with a float voltage). The solar irradiance levels of 600, 800 and 1000 W/m^2, and the temperature levels of 30, 40 and 50°C were selected to investigate the performance of the proposed battery charger control. In addition, the relationship between the voltage and current with duty-cycle control is derived using the equations as displayed below.

$$P_{out} = P_{in} \times \mathit{eff}$$

$$V_{out} I_{out} = V_{in} I_{in} \times \mathit{eff}$$

$$\mathit{Duty\ cycle} = \frac{V_{out}}{V_{in}} = \frac{I_{in}}{I_{out}} \times \mathit{eff}$$

Thus

$$\mathit{Duty\ cycle} = \frac{V_{out}}{V_{in}} \tag{1}$$

And

$$\mathit{Duty\ cycle} = \frac{I_{in}}{I_{out}} \times \mathit{eff} \tag{2}$$

where

Duty cycle is the ratio of the pulse duration, or pulse width and the period of the rectangular waveform;

P_{out} is the active power output of the battery charger;

V_{out} is the voltage output of the battery charger;

I_{out} is the current output of the battery charger;

P_{in} is the active power input of the battery charger;

V_{in} is the voltage input of the battery charger;

I_{in} is the current input of the battery charger;

eff is the efficiency of the battery charger.

– **1^{st} state of charge with constant current**

The experimental results obtained from the variation of solar irradiance levels and temperature levels are presented in Figure 12 and Figure 13, respectively. The solar irradiance levels of 600, 800, and 1000 W/m^2 are used, while the temperature is set at 37°C. To determine the effect of the temperature, the temperature levels of 30, 40, and 50°C are chosen, while the solar irradiance level is set to 800 W/m^2.

Generally, the solar energy voltage output is 34-36 V, which is higher than the charge voltage of the battery. From the results, the duty cycle can be controlled based on Equation (1) in order to regulate the charge voltage of 13-17.4 V in the constant-current charging state. In order to increase the charge efficiency, the charge current is set to 8 A with an efficiency of 83%.

Figure 12 shows the current and duty-cycle control results when the solar irradiance levels are varied. The solar irradiance levels increase, leading to a higher current and voltage being generated from solar energy. Thus, the designed solar charger needs to regulate the charge current with a constant value by controlling the duty cycle, as in Equation (2). By considering Figures 12(a), 12(b), and 12(c), the measurement results at

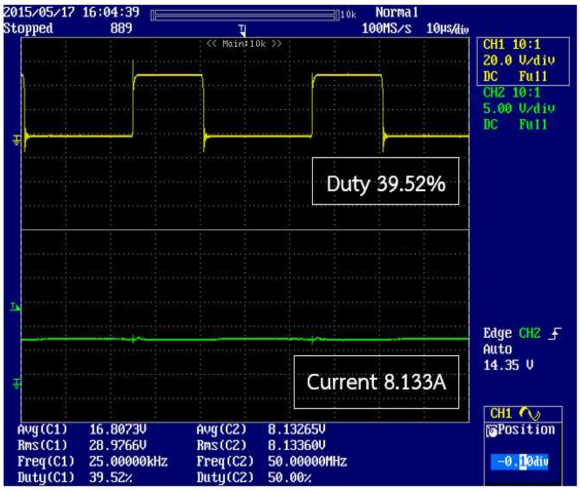

(a) Current of the charging battery with the irradiance level at 600 W/m^2

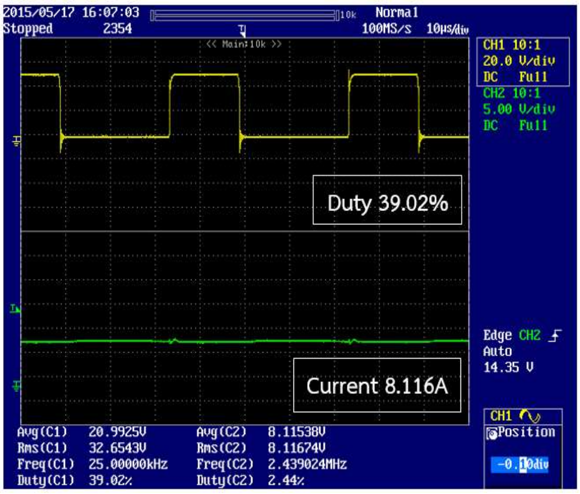

(b) Current of the charging battery with the irradiance level at 800 W/m^2

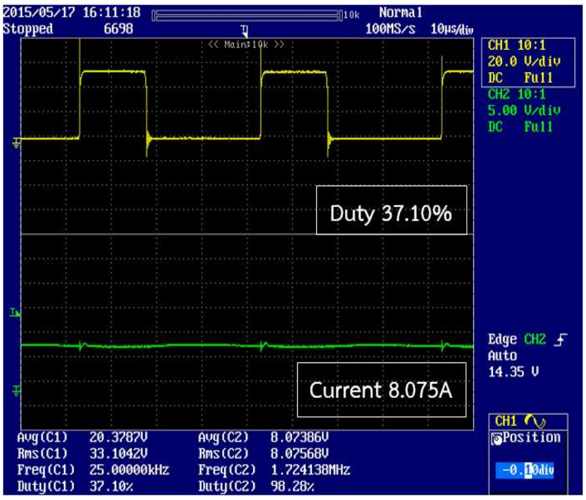

(c) Current of the charging battery with the irradiance level at 1000 W/m^2

FIGURE 12. Current and duty cycle of the charging battery while the irradiance levels are varied with a constant-current charging state

different solar irradiance levels are used to test the operation of the designed solar charger while the constant-current charging state is being activated. With respect to the effect of the temperature, as the temperature increases, the voltage and current of the solar energy output will be reduced. Therefore, the solar charger needs to regulate the charge current with a constant value for all temperature ranges.

Figures 13(a), 13(b), and 13(c) show that the designed solar charger can regulate the charge current of 8 A, which employs PWM control from the microcontroller (PIC16F87 7A) to control the duty cycle. By considering the performance of the designed solar charger operation in the constant-current charging state, the results indicate that the designed solar charger can work efficiently at different solar irradiance levels and temperature levels.

– 2nd state of charge with constant voltage

For the 2nd state, the results of the charging battery with a constant voltage, which were obtained by varying the solar irradiance level and temperature level, are illustrated in Figures 14 and 15, respectively. Solar irradiance levels of 600, 800, and 1000 W/m^2

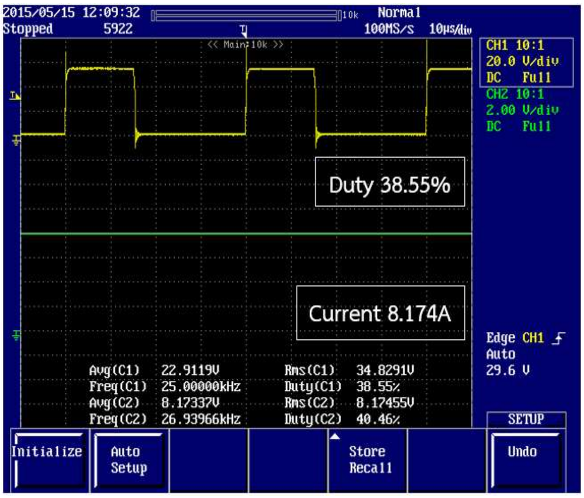

(a) Current of the charging battery with the temperature level at 30°C

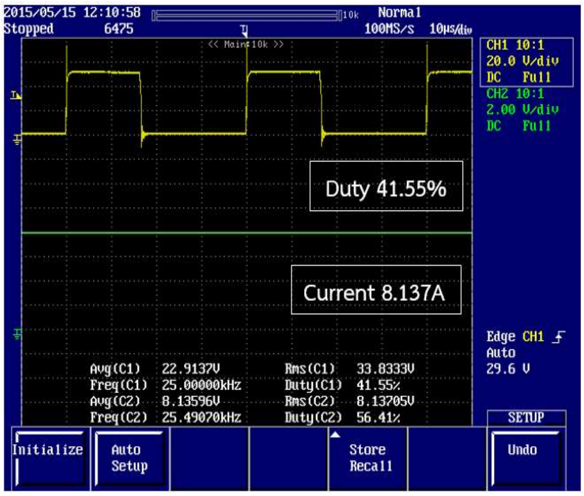

(b) Current of the charging battery with the temperature level at 40°C

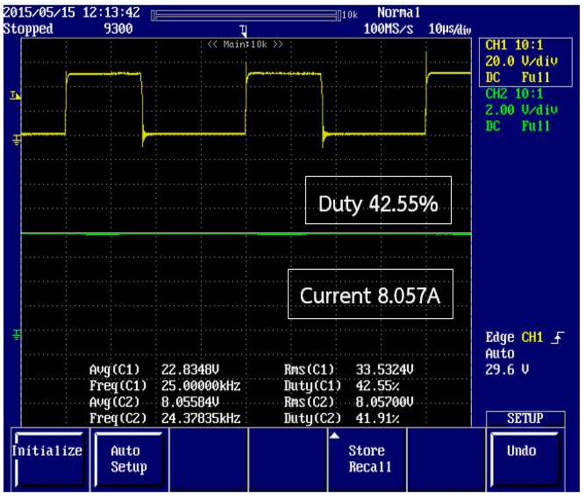

(c) Current of the charging battery with the temperature level at 50°C

FIGURE 13. Current and duty cycle of the charging battery while the temperature levels are varied with the constant-current charging state

were used, while the temperature was set to 37°C. To determine the effect of temperature, temperature levels of 30, 40, and 50°C are chosen, while the solar irradiance level is set to 800 W/m^2.

The voltage due to the solar energy is higher than the voltage used to charge the battery in the constant-voltage charging state. Thus, the solar energy voltage is regulated by employing PWM control from the microcontroller (PIC16F877A). For this reason, the charge voltage is regulated to be 14.6 V. Figure 14 shows the charge voltage and duty-cycle control of the 2nd state when the solar irradiance levels are varied. The voltage and current obtained from solar energy slightly increase, and this is caused by the increase in the solar irradiance levels. By following Equation (1), the duty cycle needs to be controlled to maintain a constant-charge voltage, which is 14.6 V. By observing Figures 14(a), 14(b) and 14(c), when the solar irradiance levels are varied, the designed solar charger can regulate the optimal charge voltage by controlling the duty cycle with the PWM control signals.

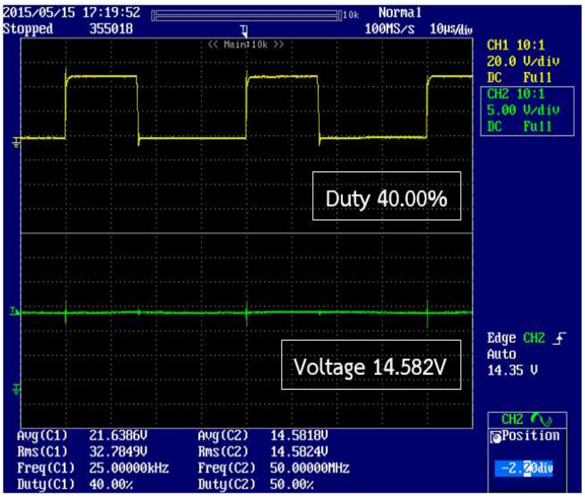

(a) Voltage of the charging battery with the irradiance level at 600 W/m^2

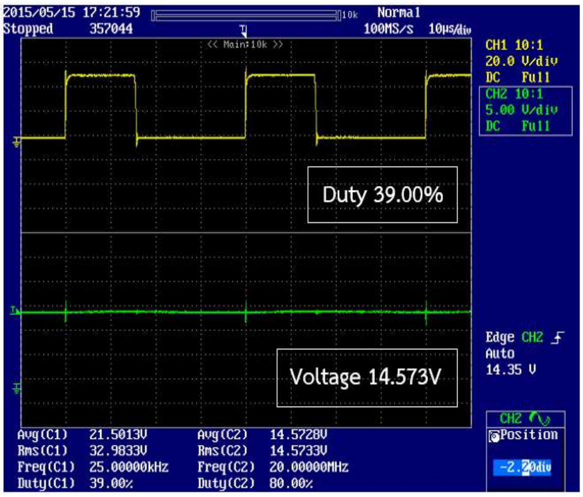

(b) Voltage of the charging battery with the irradiance level at 800 W/m^2

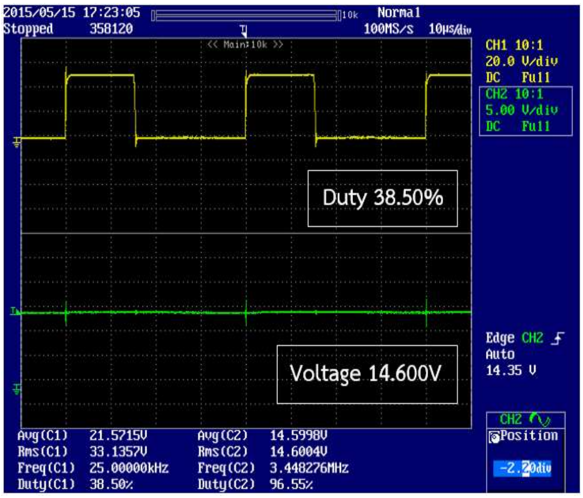

(c) Voltage of the charging battery with the irradiance level at 1000 W/m^2

FIGURE 14. Voltage and duty cycle of the charging battery while the irradiance levels are varied with the constant-voltage charging state

However, if the temperatures increase, the output voltage of the solar energy will reduce. For this reason, the designed solar charger is required to regulate the charge voltage with a constant value. Figure 15 presents voltage regulation results which were obtained by varying the temperature levels. When the temperature levels increase by considering Figures 15(a), 15(b) and 15(c), the duty cycle is controlled by the microcontroller to increase according to Equation (1) in order to regulate the charge voltage of 14.6 V. It can be seen that the designed solar charger operates efficiently in the constant-voltage charging state with different solar irradiance levels and temperature levels.

– **3rd state of charge with float voltage**

For the last state of charge, the float-voltage charging state is activated by controlling the microcontroller. The voltage of this stage is set to be 13.8 V until the charging current decreases to 0.1 A, which is the same as the fully charged battery; the battery will be cut off, so it will not deliver current to the solar energy source. In order to test the performance of this float-voltage charge, the results of the solar irradiance level and

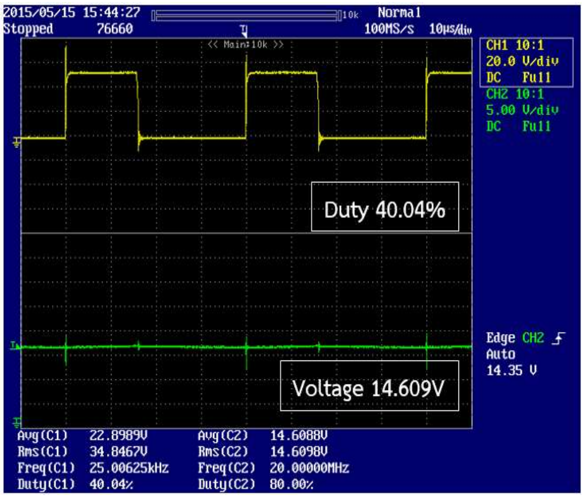

(a) Voltage of the charging battery with the temperature level at 30°C

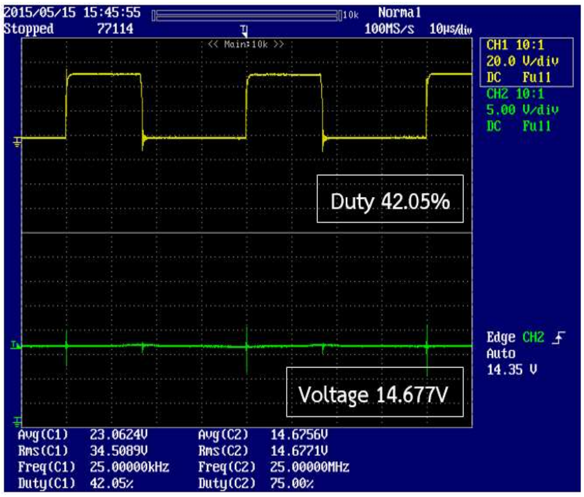

(b) Voltage of the charging battery with the temperature level at 40°C

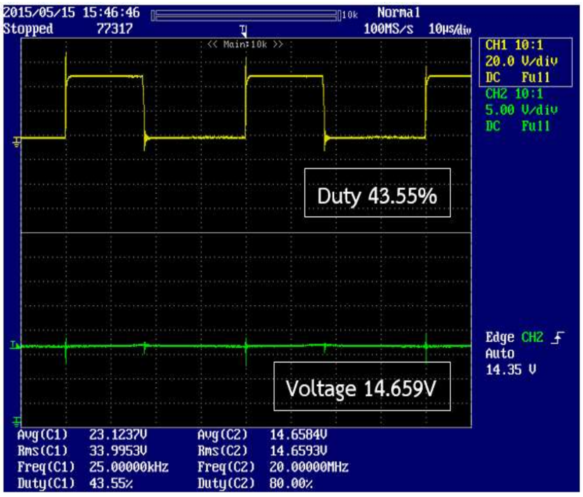

(c) Voltage of the charging battery with the temperature level at 50°C

FIGURE 15. Voltage and duty cycle of the charging battery while the temperature levels are varied with the constant-voltage charging state

temperature level variation are illustrated in Figure 16 and Figure 17, respectively. Solar irradiance levels of 600, 800, and 1000 W/m^2 are used, while the temperature is set to 37°C. To determine the effect of the temperature, the temperature values of 30, 40, and 50°C are chosen, while the solar irradiance level is set to 800 W/m^2.

As discussed above, both the solar irradiance levels and temperature levels directly affect the voltage and current output of the solar energy. For this reason, the designed solar charger needs to regulate the suitable float-voltage charging under different environmental conditions. When the solar irradiance levels are varied by considering Figures 16(a), 16(b) and 16(c), the charge voltage of 13.8 V is regulated by employing PWM control using the switching of the microcontroller to control the duty cycle. Likewise, the results of the temperature-level variation in Figures 17(a), 17(b) and 17(c) show that it efficiently controls the duty cycle. It is found that the designed solar charger can efficiently regulate the charge voltage in the float-voltage charging state under different environmental conditions.

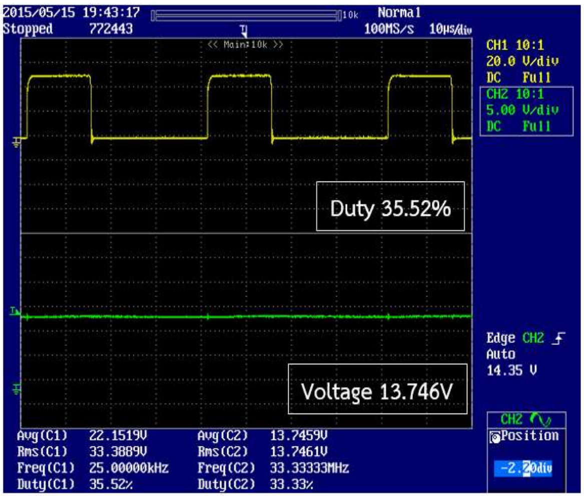

(a) Voltage of the charging battery with the irradiance level at 600 W/m^2

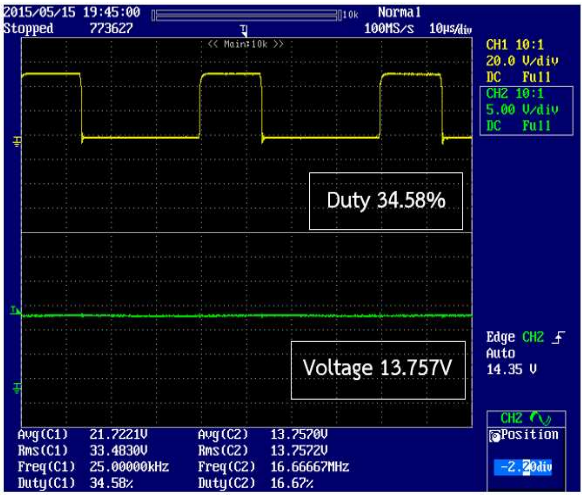

(b) Voltage of the charging battery with the irradiance level at 800 W/m^2

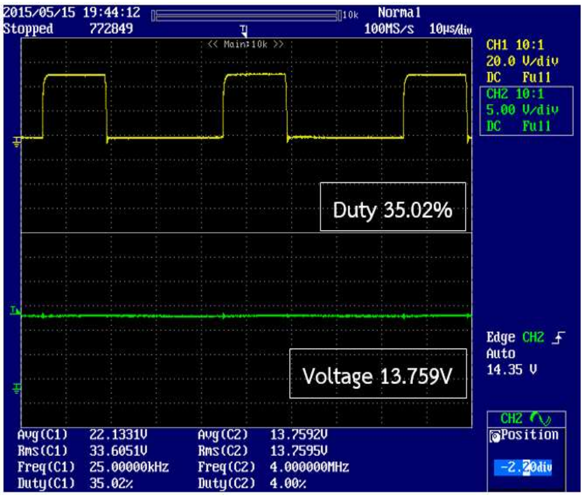

(c) Voltage of the charging battery with the irradiance level at 1000 W/m^2

FIGURE 16. Voltage and duty cycle of the charging battery while the irradiance levels are varied in the float-voltage charging state

5. **Conclusions.** This paper presented the design of a solar energy battery charger which consists of three charging states: a constant-current charging state, a constant-voltage charging state and a float-voltage charging state. A 12-V 60-Ah lead-acid battery was used to test the designed battery charger, and a PV simulator was used to simulate a 160-W solar panel, considering irradiance and temperature conditions.

– The constant-current charging state has limitations in terms of the charging current, which ranges between the minimum rating of 0.1 C and the maximum rating of 0.25 C. If the battery charge exceeds the range of the determined current, the battery lifespan will decrease. For this case study, a charging current of 8 A was selected, and therefore the battery terminal voltage of the battery was 14.6 V.

– The constant-voltage charging state is employed to control the constant voltage at the rated charged value of 14.6 V. After that, the charging current decreases as the charging voltage reaches the battery terminal voltage. When the charging current decreased to 1.5 A, the system shifts to the third charging state.

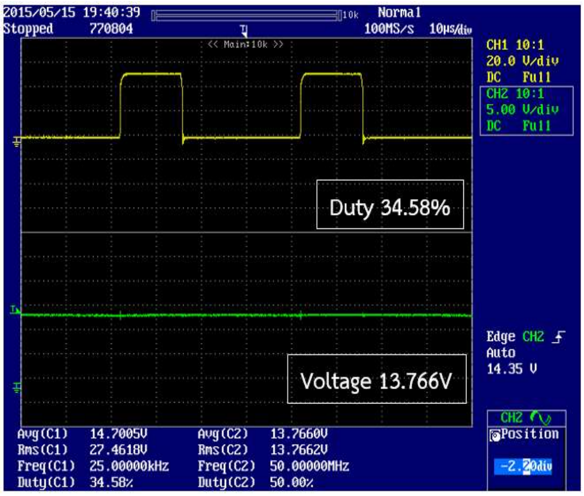

(a) Voltage of the charging battery with the temperature level at 30°C

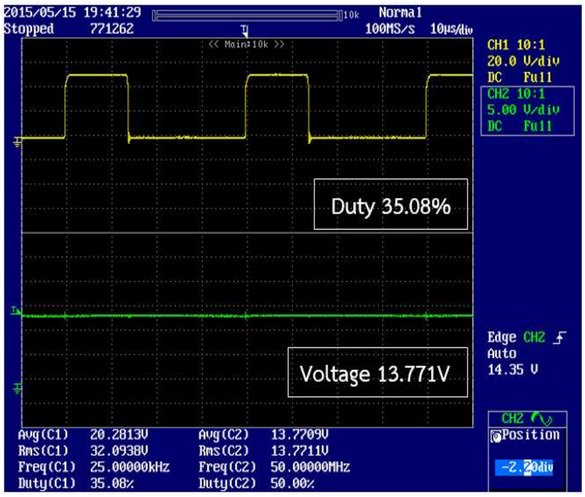

(b) Voltage of the charging battery with the temperature level at 40°C

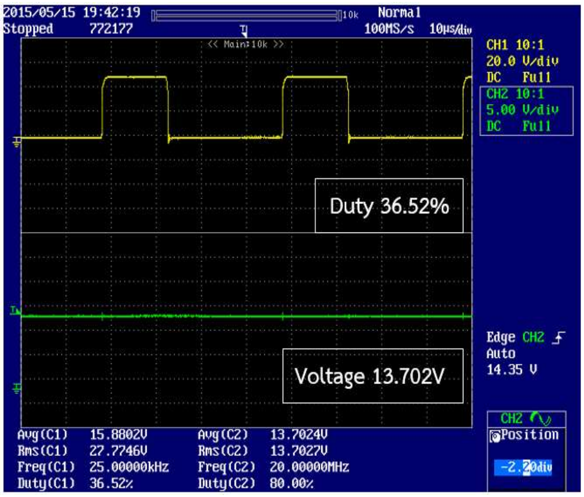

(c) Voltage of the charging battery with the temperature level at 50°C

FIGURE 17. Voltage and duty cycle of the charging battery while the temperature levels are varied in the float-voltage charging state

– The float-voltage charging state is the last charging state which provides the charging voltage as well as the battery terminal voltage, which is 13.8 V. The charging current value approaches zero, which indicates that the battery is fully charged. The designed battery charger disconnects the solar energy source to prevent overvoltage conditions, which would result degraded battery performance and severely reduced lifespan.

The control of the battery charging during each charging state is based on the power circuit and the control circuit. A microcontroller was employed to process and control the changes in the charging states to a suitable voltage and current at various solar irradiance levels and temperature levels, hence increasing the lifetime of the battery. However, the lead-acid battery has the limitation of slow charge, low specific energy, and needs to be stored in the charged condition. For future work, a hybrid energy-storage solar energy charger is proposed and designed to deal with the limitations of the lead-acid battery. Hybrid energy-storage alternatives to be studied include lithium-ion batteries and lead-acid batteries, as well as supercapacitors and lead-acid batteries.

Acknowledgment. The work presented in this paper is part of a research project (No. 2559-01-01024) sponsored by the Faculty of Engineering, King Mongkut's Institute of Technology Ladkrabang Research Fund. The author would like to thank them for the financial support.

REFERENCES

[1] L. G. Thomas and A. K. Nelson, Solar photovoltaic charging of lithium-ion batteries, *J. Power Sources*, vol.195, no.12, pp.3928-3932, 2010.
[2] *Battery and Energy Technologies Website*, http://www.mpoweruk.com.
[3] A. A. Hussein and A. A. Fardoun, Design considerations and performance evaluation of outdoor PV battery chargers, *Renewable Energy*, vol.82, pp.85-91, 2015.
[4] K. Eguchi, T. Junsing, A. Julsereewong, W. Do and I. Oota, Design of a nesting-type switched-capacitor AC/DC converter using voltage equalizers, *International Journal of Innovative Computing, Information and Control*, vol.13, no.4, pp.1369-1384, 2017.
[5] R. C. Cope and Y. Podrazhansky, The art of battery charging, *Proc. of the 14th Annual Battery Conference on Applications and Advances*, Long Beach, CA, pp.233-235, 1999.
[6] S. Li, C. Zhang and S. Xie, Research on fast charge method for lead-acid electric vehicle batteries, *International Workshop on Intelligent Systems and Applications*, Wuhan, China, pp.1-5, 2009.
[7] Y. Guo and C. Zhang, Study on the fast charging method of lead-acid battery with negative pulse discharge, *The 4th International Conference on Power Electronics Systems and Applications*, Hong Kong, pp.1-4, 2011.
[8] A. Al-Haj Hussein and I. Batarseh, A review of charging algorithms for nickel and lithium battery chargers, *IEEE Trans. Vehicular Technology*, vol.60, no.3, pp.830-838, 2011.
[9] F. Boico, B. Lehman and K. Shujaee, Solar battery chargers for NiMH batteries, *IEEE Trans. Power Electronics*, vol.22, no.5, pp.1600-1609, 2007.
[10] J. Yan, G. Xu, H. Qian, Y. Xu and Z. Song, Model predictive control-based fast charging for vehicular batteries, *Energies*, vol.4, pp.1178-1196, 2011.
[11] H. I. Hsieh, C. Y. Tsai and G. C. Hsieh, Photovoltaic burp charge system on energy-saving configuration by smart charge management, *IEEE Trans. Power Electronics*, vol.29, no.4, pp.1777-1790, 2014.
[12] W. Li, X. Lv, Y. Deng, J. Liu and X. He, A review of non-isolated high step-up DC/DC converters in renewable energy applications, *The 24th Annual IEEE Applied Power Electronics Conference and Exposition*, Washington, DC, pp.364-369, 2009.
[13] Q. Li and P. Wolfs, A review of the single phase photovoltaic module integrated converter topologies with three different DC link configurations, *IEEE Trans. Power Electronics*, vol.23, no.3, pp.1320-1333, 2008.
[14] C. Chen, C. Wang and F. Hong, Research of an interleaved boost converter with four interleaved boost convert cells, *Asia Pacific Conference on Postgraduate Research in Microelectronics & Electronics (PrimeAsia)*, Shanghai, China, pp.396-399, 2009.
[15] H. Fathabadi, Novel photovoltaic based battery charger including novel high efficiency step-up DC/DC converter and novel high accurate fast maximum power point tracking controller, *Energy Conversion and Management*, vol.110, pp.200-211, 2016.
[16] S. H. Park, S. R. Park, J. S. Yu, Y. C. Jung and C. Y. Won, Analysis and design of a soft-switching boost converter with an HI-bridge auxiliary resonant circuit, *IEEE Trans. Power Electronics*, vol.25, no.8, pp.2142-2149, 2010.
[17] W. Y. Choi, S. M. Kim, S. J. Park, K. H. Kim and Y. C. Lim, High step-up DC-DC converter with high efficiency for photovoltaic module integrated converter systems, *The 31st International Telecommunications Energy Conference*, Incheon, Korea, pp.1-4, 2009.
[18] E. Koutroulis, K. Kalaitzakis and N. C. Voulgaris, Development of a microcontroller-based, photovoltaic maximum power point tracking control system, *IEEE Trans. Power Electronics*, vol.16, no.1, pp.46-54, 2001.
[19] M. P. Alberto, A. Jorge, J. P. Miguel and A. M. Juan, A modular strategy for isolated photovoltaic systems based on microcontroller, *Renewable Energy*, vol.34, pp.1825-1832, 2009.
[20] V. Salas, A. Olias and A. Barrado, Evaluation of a new maximum power point tracker (MPPT) applied to the photovoltaic stand-alone systems, *Solar Energy Materials & Solar Cells*, vol.87, pp.807-815, 2005.

[21] L. Khemissi, B. Khiari, R. Andoulsi and A. Cherif, Low cost and high efficiency of single phase photovoltaic system based on microcontroller, *Solar Energy*, vol.86, no.5, pp.1129-1141, 2012.
[22] Y. C. Kuo, Y. J. Luo and L. J. Liu, Synthesizable integrated circuit and system design for solar chargers, *IEEE Trans. Power Electronics*, vol.28, no.9, pp.4260-4266, 2013.
[23] J. López, S. I. Seleme Jr., P. F. Donoso, L. M. F. Morais, P. C. Cortizo and M. A. Severo, Digital control strategy for a buck converter operating as a battery charger for stand-alone photovoltaic systems, *Solar Energy*, vol.140, pp.171-187, 2016.
[24] Y. E. A. Eldahab, N. H. Saad and A. Zekry, Enhancing the design of battery charging controllers for photovoltaic systems, *Renewable and Sustainable Energy Reviews*, vol.58, pp.646-655, 2016.